Article

# Cyano- and Isocyanotris(trifluoromethyl)borates: Syntheses, Spectroscopic Properties, and Solid State Structures of K[(CF)BCN] and K[(CF)BNC]

Maik Finze, Eduard Bernhardt, Helge Willner, and Christian W. Lehmann

*J. Am. Chem. Soc.*, **2005**, 127 (30), 10712-10722• DOI: 10.1021/ja0516357 • Publication Date (Web): 07 July 2005



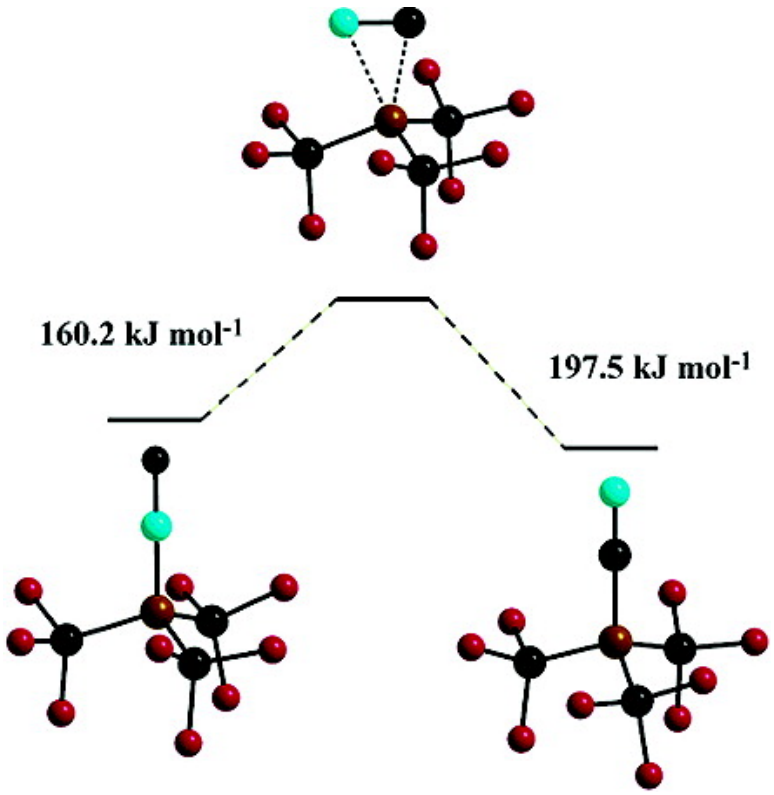


## More About This Article

Additional resources and features associated with this article are available within the HTML version:

- Supporting Information
- Links to the 4 articles that cite this article, as of the time of this article download
- Access to high resolution figures
- Links to articles and content related to this article

J|A|C|S
ARTICLES
Published on Web 07/07/2005

# Cyano- and Isocyanotris(trifluoromethyl)borates: Syntheses, Spectroscopic Properties, and Solid State Structures of $K[(CF_3)_3BCN]$ and $K[(CF_3)_3BNC]$

Maik Finze,*[,†,§] Eduard Bernhardt,[†] Helge Willner,*[,†] and Christian W. Lehmann*[,‡]

*Contribution from the FBC - Anorganische Chemie, Bergische Universität Wuppertal, Gaussstrasse 20, D-42097 Wuppertal, Germany, and Max-Planck-Institut für Kohlenforschung, Kaiser-Wilhelm-Platz 1, D-45470 Mülheim an der Ruhr, Germany*

Received April 6, 2005; E-mail: lehmann@mpi-muelheim.mpg.de; maik.finze@uni-duesseldorf.de; willner@uni-wuppertal.de

***Abstract:*** A two step synthesis to the isocyanotris(trifluoromethyl)borate anion, $[(CF_3)_3BNC]^-$, and its isomerization to the cyanotris(trifluoromethyl)borate anion, $[(CF_3)_3BCN]^-$, at temperatures above 150 °C are presented. In the first step $(CF_3)_3BNCH$ was obtained by reacting $(CF_3)_3BCO$ with hydrogen cyanide followed by deprotonation of the HCN adduct with $Li[N(SiMe_3)_2]$ in toluene. The thermal behavior of $K[(CF_3)_3BNC]$ and $K[(CF_3)_3BCN]$ were investigated by differential scanning calorimetry (DSC), and $K[BF_4]$ was identified as a major solid decomposition product. The enthalpy of the isocyanide−cyanide rearrangement, $\Delta H_{iso} = -35 \pm 4$ kJ mol$^{-1}$, was obtained from DSC measurements, and the activation energy, $E_a = 180 \pm 20$ kJ mol$^{-1}$, from kinetic measurements. The isomerization was modeled as an intramolecular reaction employing DFT calculations at the B3LYP/6-311+G(d) level of theory yielding a reaction enthalpy of $\Delta H_{iso} = -36.1$ kJ mol$^{-1}$ and an activation energy of $E_a = 155.7$ kJ mol$^{-1}$. The solid-state structures of $K[(CF_3)_3BNC]$ and $K[(CF_3)_3BCN]$ were determined by single-crystal X-ray diffraction. Both salts are isostructural and crystallize in the orthorhombic space group *Pnma* (no. 62). In the crystals the borate anions possess $C_s$ symmetry, while for the energetic minimum $C_3$ symmetry is predicted by DFT calculations. The borate anions have been characterized by IR and Raman spectroscopy as well as by NMR spectroscopy. The assignment of the IR and Raman bands is supported by their calculated wavenumbers and intensities. The spectroscopic and structural properties of both borate anions are compared to the properties of the isoelectronic borane carbonyl $(CF_3)_3BCO$ and the $[B(CF_3)_4]^-$ anion as well as to those of other related species.

## Introduction

Since the synthesis of the first cyanoborate anion $[H_3BCN]^-$ in 1951,[1] many other cyanoboron derivatives have been obtained by different routes, e.g., $[H_2B(CN)_2]^-$,[2−4] $[HB(CN)_3]^-$,[3] $[B(CN)_4]^-$,[5−8] $[F_nB(CN)_{4-n}]^-$,[7,9] and $[(C_6F_5)_3BCN]^-$.[10] In contrast to cyanoboron compounds there are only a few reports on isocyanoborates and -boranes. The first examples were *o*-$C_2B_{10}H_{11}$-3-NC in 1970, which was obtained by dehydration of *o*-$C_2B_{10}H_{11}$-3-NHC(O)H,[11,12] and $[H_nB(NC)_{4-n}]^-$ ($n = 1, 2$) as a mononuclear boron species in 1983 by release from the corresponding Ag(I) complexes with sodium.[3,13] *o*-$C_2H_2B_{10}H_9$-3-NC is converted to the respective cyano isomer at 250−300 °C,[11] and $[H_nB(NC)_{4-n}]^-$ rearranges to $[H_nB(CN)_{4-n}]^-$ ($n = 1$, 2) in boiling dibutyl ether (142 °C).[3] Neither investigations on the kinetics of the isomerizations nor theoretical studies have been published, so far.

In contrast to these rare examples for isocyanide−cyanide isomerizations in boron chemistry, in organic chemistry a substantial number of isocyanide−cyanide rearrangements have been reported.[14,15] The first example was discovered as early as 1873: the isomerization of phenylisocyanide to phenylcyanide.[16] Furthermore the conversion of isonitriles into the corresponding nitriles has evolved to a valuable synthetic route for nitriles.[14,15] In some cases the enthalpies and activation

[†] Bergische Universität Wuppertal.
[‡] Max-Planck-Institut für Kohlenforschung.
[§] Present address: Institut für Anorganische Chemie und Strukturchemie II, Heinrich-Heine-Universität Düsseldorf, Universitätsstrasse 1, D-40225 Düsseldorf, Germany.

(1) Wittig, G.; Raff, Z. *Z. Naturforsch., B: Chem. Sci.* **1951**, *6*, 225.
(2) Emri, J.; Györi, B. *J. Chem. Soc., Chem. Commun.* **1983**, 1303.
(3) Györi, B.; Emri, J.; Fehér, I. *J. Organomet. Chem.* **1983**, *255*, 17.
(4) Spielvogel, B. F.; Ahmed, F. U.; Das, M. K.; McPhail, A. T. *Inorg. Chem.* **1984**, *23*, 3263.
(5) Bernhardt, E.; Henkel, G.; Willner, H. *Z. Anorg. Allg. Chem.* **2000**, *626*, 560.
(6) Williams, D.; Pleune, B.; Kouvetakis, J.; Williams, M. D.; Andersen, R. A. *J. Am. Chem. Soc.* **2000**, *122*, 7735.
(7) Bernhardt, E.; Berkei, M.; Schürmann, M.; Willner, H. *Z. Anorg. Allg. Chem.* **2003**, *629*, 677.
(8) Bernhardt, E.; Finze, M.; Willner, H. *Z. Anorg. Allg. Chem.* **2003**, *629*, 1229.
(9) Hamilton, B. H.; Ziegler, C. J. *J. Chem. Soc., Chem. Commun.* **2002**, 842.
(10) Vei, I. C.; Pascu, S. I.; Green, M. L. H.; Green, J. C.; Schilling, R. E.; Anderson, G. D. W.; Rees, L. H. *J. Chem. Soc., Dalton Trans.* **2003**, 2550.
(11) Zakharkin, L. I.; Kalinin, V. N.; Gedymin, V. V.; Dzarasova, G. S. *J. Organomet. Chem.* **1970**, *23*, 303.
(12) Zakharkin, L. I.; Kalinin, V. N.; Gedymin, V. V. *Bulletin of the Academy of Sciences of the USSR/Division of Chemistry* **1970**, *19*, 1157.
(13) Györi, B.; Berente, Z.; Lázár, I. *Polyhedron* **1998**, *17*, 3175.
(14) Maloney, K. M.; Rabinovitch, B. S. In *Isonitrile Chemistry*; Ugi, I., Ed.; Academic Press: New York, 1971; p 41.
(15) Rüchardt, C.; Meier, M.; Haaf, K.; Pakusch, J.; Wolber, E. K. A.; Müller, B. *Angew. Chem.* **1991**, *103*, 907.
(16) Weith, W. *Ber. Dtsch. Chem. Ges.* **1873**, *6*, 210.


**10.1021/ja0516357 CCC: $30.25** 

energies of the isomerizations have been determined, for example, for MeNC/MeCN[17,18] or for $C_6H_5CH_2NC/C_6H_5CH_2CN$.[19]

Recently we have reported the synthesis of carbonyltris(trifluoromethyl)borane, $(CF_3)_3BCO$, in a three-step synthesis starting from easily accessible chemicals according to eq 1 with an overall yield of 34%.[20, 21]

$$[BF_4]^- \xrightarrow[\Delta,\ 60\%]{KCN/LiCl} [B(CN)_4]^- \xrightarrow[-40\ °C \rightarrow rt,\ 64\%]{ClF_3/aHF} [B(CF_3)_4]^- \xrightarrow[rt,\ 88\%]{H_2SO_4} (CF_3)_3BCO \quad (1)$$

The structural, spectroscopic, and thermal properties as well as the decomposition pathway of $(CF_3)_3BCO$ were investigated in detail, and the studies were supported by DFT calculations.[21,22] Especially the unexpected strong B−CO bond (experimental, 112 kJ mol$^{-1}$; calculated, 114 kJ mol$^{-1}$)[21,22] and the highly electrophilic C atom, due to the high Lewis acidity of $(CF_3)_3B$,[22] make $(CF_3)_3BCO$ an ideal starting material for the synthesis of compounds with the tris(trifluoromethyl)boron group. The borane carbonyl reacts with nucleophiles either under addition to the C atom of the carbonyl ligand, examples being the syntheses $K[(CF_3)_3BC(O)F]$,[23] $[Ph_4P][(CF_3)_3BC(O)Hal]$ (*Hal* = Cl, Br, I),[24] and $[Pr_3NH][(CF_3)_3BC(O)OH]$,[21] or in ligand exchange reactions under loss of carbon monoxide, e.g., the formations of $(CF_3)_3BNCMe$,[21] $[Co(CO)_5][(CF_3)_3BF]$,[25] and $K[(CF_3)_3BF]$.[22]

In this contribution we report on (i) the synthesis of the isocyanoborate $K[(CF_3)_3BNC]$ using the so far unknown adduct $(CF_3)_3BNCH$ as starting material, (ii) its thermal isomerization yielding $K[(CF_3)_3BCN]$, (iii) their thermal properties determined by differential scanning calorimetry (DSC), (iv) the experimental and calculated (DFT) activation energy ($E_a$) and enthalpy of the isomerization ($\Delta H_{iso}$), (v) the structures of $K[(CF_3)_3BNC]$ and $K[(CF_3)_3BCN]$ determined by single-crystal X-ray diffraction, (vi) the vibrational analysis of both borate anions supported by DFT calculations, and (vii) a comprehensive characterization of $(CF_3)_3BNCH$, $K[(CF_3)_3BNC]$, and $K[(CF_3)_3BCN]$ by multinuclear NMR methods.

In a short communication we have recently reported on the syntheses of $[(CF_3)_3BCPnic]^-$ (*Pnic* = P, As) as $[PPh_4]^+$ salts,[26] which are isovalence electronic to $[(CF_3)_3BCN]^-$. A comprehensive comparison of their thermal, spectroscopic, and structural properties to those of cyanotris(trifluoromethyl)borates will be reported elsewhere.

## Experimental Section

**General Procedures and Reagents. (a) Apparatus.** Volatile materials were manipulated in glass vacuum lines of known volume equipped with valves with PTFE stems (Young, London) and with capacitance pressure gauges (Type 280E, Setra Instruments, Acton, MA and 221 AHS-1000, MKS Baratron, Burlington, MA). The reactions involving air-sensitive compounds were performed under a $N_2$ or Ar atmosphere using standard Schlenk line techniques. Solid materials were manipulated inside an inert atmosphere box (Braun, Munich, Germany) filled with argon, with a residual moisture content of less than 1 ppm. Volatile compounds were stored in flame-sealed glass ampules under liquid nitrogen in a storage Dewar vessel. The ampules were opened and flame-sealed using an ampule key.[27]

**(b) Chemicals.** $(CF_3)_3BCO$ was synthesized as described previously from $K[B(CF_3)_4]$.[20,21] HCN and $HC^{15}N$ were synthesized from KCN (>96%, Merck KGaA) and $KC^{15}N$ (99% $^{15}N$ enrichment, Cambridge Isotopes) with concentrated sulfuric acid. $Li[N(SiMe_3)_2]$ was obtained from Aldrich. All dry solvents were obtained from Aldrich and transferred under a $N_2$ or Ar atmosphere into 1 L round-bottom flasks equipped with valves with PTFE stems (Young, London) and charged with molecular sieves (4 Å). All other chemicals were obtained from commercial sources and used as received.

**(c) Synthetic Reactions. (1) $(CF_3)_3BNCH$.** A 50 mL round-bottom flask equipped with a valve with a PTFE stem (Young, London), fitted with a PTFE-coated magnetic stirring bar, was charged with 2.04 g (8.3 mmol) of $(CF_3)_3BCO$. About 20 mL dry $CH_2Cl_2$ were condensed in vacuo, into the flask, kept at −196 °C followed by 13.1 mmol HCN. The reaction mixture was placed into a cold bath kept at −78 °C and allowed to warm to room temperature overnight under vigorous stirring. All volatile materials were removed under reduced pressure, and an off-white solid was obtained (1.94 g, 96%). Anal. Calcd for $C_4HBF_9N$: C, 19.62; H, 0.41; N, 5.72. Found: C, 19.80; H, 0.40; N, 5.80.

**(2) $K[(CF_3)_3BNC]$.** $(CF_3)_3BNCH$ (1.12 g, 4.6 mmol) was placed into a 100 mL Schlenk reactor and fitted with a PTFE-coated magnetic stirring bar. A 50 mL round-bottom flask equipped with a valve with a PTFE stem (Young, London) was charged with 1.92 g (11.5 mmol) of $Li[N(SiMe_3)_2]$. Both solids were dissolved in 40 mL of dry toluene. The amide solution was cannula transferred into a 100 mL dropping funnel placed on top of the Schlenk reactor containing the $(CF_3)_3BNCH$ solution. The reaction vessel was cooled to −20 °C, and under vigorous stirring the amide solution was added dropwise at −20 °C over a period of 2 h. Immediately after addition of the first amount of $Li[N(SiMe_3)_2]$/toluene a white solid precipitated from the reaction mixture. After complete addition the mixture was stirred for further 30 min at −20 °C. KOH/$H_2O$ solution (20 mL) was added to the reaction mixture. The toluene layer was separated, and the toluene was removed in vacuo. The residue of the toluene phase was dissolved in diethyl ether and subsequently added to the KOH solution. $K_2CO_3$ (0.5 g) and $Et_2O$ (150 mL) were added to the reaction mixture. The ethereal layer was separated, and the residue was extracted twice with diethyl ether (100 mL, 50 mL). The combined organic layers were dried with $K_2CO_3$. All volatiles were removed in vacuo, and an off-white solid was obtained (1.08 g, 84%). Anal. Calcd for $C_4BF_9KN$: C, 16.98; N, 4.95. Found: C, 17.11; N, 5.10.

**(3) $K[(CF_3)_3BCN]$.** A small glass vial ($V \approx 2$ mL) was charged with 515 mg (1.8 mmol) of $K[(CF_3)_3BNC]$ and placed into the heating chamber of our DSC instrument. The sample was held at 200−240 °C for 10 min. The off-white solid (515 mg, 100%) was cooled to room temperature. Anal. Calcd for $C_4BF_9KN$: C, 16.98; N, 4.95. Found: C, 16.79; N, 4.97.

**(4) $K[(CF_3)_3BNHC(O)H]$.** $K[(CF_3)_3BNC]$ (250 mg, 0.9 mmol) was placed into a 20 mL beaker, fitted with a PTFE-coated magnetic stirring bar, and dissolved in 3 mL of water. Approximately 3 mL of concentrated hydrochloric acid were added to the vigorously stirred solution, and the reaction mixture was stirred for further 10 min. All volatile compounds were removed under reduced pressure, and the resulting colorless material was taken up into 10 mL of $Et_2O$.

(17) Schneider, F. W.; Rabinovitch, B. S. *J. Am. Chem. Soc.* **1962**, *84*, 4215.
(18) Baghal-Vayjooee, M. H.; Colister, J. L.; Pritchard, H. O. *Can. J. Chem.* **1977**, *55*, 2634.
(19) Meier, M.; Müller, B.; Rüchardt, C. *J. Org. Chem.* **1987**, *52*, 648.
(20) Terheiden, A.; Bernhardt, E.; Willner, H.; Aubke, F. *Angew. Chem., Int. Ed.* **2002**, *41*, 799.
(21) Finze, M.; Bernhardt, E.; Terheiden, A.; Berkei, M.; Willner, H.; Christen, D.; Oberhammer, H.; Aubke, F. *J. Am. Chem. Soc.* **2002**, *124*, 15385.
(22) Finze, M.; Bernhardt, E.; Zähres, M.; Willner, H. *Inorg. Chem.* **2004**, *43*, 490.
(23) Finze, M.; Bernhardt, E.; Willner, H.; Lehmann, C. W. *Angew. Chem., Int. Ed.* **2003**, *42*, 1052.
(24) Finze, M.; Bernhardt, E.; Lehmann, C. W.; Willner, H. *Chem. Eur. J.*, in press.
(25) Bernhardt, E.; Finze, M.; Willner, H.; Lehmann, C. W.; Aubke, F. *Angew. Chem.* **2004**, *116*, 4254.
(26) Finze, M.; Bernhardt, E.; Willner, H.; Lehmann, C. W. *Angew. Chem., Int. Ed.* **2004**, *43*, 4159.
(27) Gombler, W.; Willner, H. *J. Phys. E: Sci. Instrum.* **1987**, *20*, 1286.

***Table 1.*** Crystallographic Data of $K[(CF_3)_3BCN]$ and $K[(CF_3)_3BNC]$ at 100 K

| compound | $K[(CF_3)_3BCN]$ | $K[(CF_3)_3BNC]$ |
|---|---|---|
| empirical formula | $C_4BF_9KN$ | $C_4BF_9KN$ |
| formula weight [g mol$^{-1}$] | 282.96 | 282.96 |
| crystal system, space group | orthorhombic, *Pnma* (no. 62) | orthorhombic, *Pnma* (no. 62) |
| unit cell dimensions | | |
| *a* [Å] | 9.6479(1) | 9.7507(2) |
| *b* [Å] | 10.4721(2) | 10.4377(2) |
| *c* [Å] | 9.3000(2) | 9.2776(2) |
| unit cell volume *V* [Å$^3$] | 939.61(3) | 944.23(3) |
| *Z* value | 4 | 4 |
| $\rho_{calc}$ [Mg m$^{-3}$] | 2.000 | 1.990 |
| $R_1$, $[I > 2\sigma(I)]^a$ | 0.0321 | 0.0300 |
| $R_1$,[a] all data | 0.0404 | 0.0387 |
| $wR_2$,[b] all data | 0.0816 | 0.0656 |

[a] $R_1 = (\sum||F_o| - |F_c||)/\sum|F_o|$. [b] $R_w = [\sum w(F_o^2 - F_c^2)^2/\sum wF_o^2]^{1/2}$, weight scheme $w = [\sigma^2(F_o) + (aP)^2 + bP]^{-1}$; $P = (\max(0,F_o^2) + 2F_c^2)/3$; ($K[(CF_3)_3BCN]$: $a = 0.0323$, $b = 0.3273$. $K[(CF_3)_3BNC]$: $a = 0.0201$, $b = 0.4636$).

Concentrated $K_2CO_3/H_2O$ solution (1 mL) was added to the ethereal phase and stirred for a few minutes. $K_2CO_3$ was added until the water layer became solid. The ethereal layer was separated, and the residue in the beaker was washed 2 times with 5 mL of $Et_2O$. The organic phases were combined, and all volatile materials were removed in vacuo. The beige solid was dissolved in $CD_3CN$ and studied by NMR spectroscopy.

**(5) $(CF_3)_3B^{15}NCH$, $K[(CF_3)_3B^{15}NC]$, $K[(CF_3)_3BC^{15}N]$, and $K[(CF_3)_3B^{15}NHC(O)H]$.** The isotopical labeled compounds were synthesized by the same procedures as described for the nonlabeled compounds.

**(6) Determination of the Isomerization Rate and the Enthalpy of Conversion of $K[(CF_3)_3BNC]$ into $K[(CF_3)_3BCN]$.** Samples of $K[(CF_3)_3BNC]$ were filled into melting point capillaries and heated in an oil bath. The rate of conversion was monitored by Raman spectroscopy via the intensities of the CN stretching bands. The ratios of the Raman activities were corrected to the molar ratios by reference values derived from $^{19}F$ NMR spectroscopy: $I_{Ra}(K[(CF_3)_3BCN])/I_{Ra}(K[(CF_3)_3BNC])\cdot R^{-1} = I_{NMR}(K[(CF_3)_3BCN])/I_{NMR}(K[(CF_3)_3BNC])$; $R = 1.19$. The reaction rates were determined at four different temperatures (139, 156, 164, and 171 °C). Using these values enabled the calculation of the activation energy ($E_a$) using Arrhenius' equation.

**(d) Instrumentation. (I) Single-Crystal X-ray Diffraction.** Crystals suitable for X-ray diffraction were obtained by slow diffusion of dichloromethane into a diethyl ether solution. Diffraction data were collected at 100 K on a KappaCCD diffractometer (Bruker AXS) using Mo $K_\alpha$ radiation ($\lambda = 0.710\,73$ Å) and a graphite monochromator. Crystal structures were determined using SHELXS-97,[28] and full-matrix least-squares refinements based on $F^2$ were performed using SHELXL-97.[29] Integration and empirical absorption corrections (DENZO scalepack)[30] were applied. Molecular structure diagrams were drawn using the program Diamond.[31] A summary of experimental details and crystal data is collected in Table 1.

**(II) Vibrational Spectroscopy.** Infrared spectra were recorded at room temperature on an IFS 66v FTIR instrument (Bruker, Karlsruhe, Germany). A DTGS detector, together with a KBr/Ge beam splitter, was used in the region 5000−400 cm$^{-1}$, and a Ge-coated 6 $\mu$m Mylar beam splitter and a far-IR DTGS detector were used in the region 650−80 cm$^{-1}$. Raman spectra were recorded on a Bruker RFS 100/S FT Raman spectrometer using the 1064 nm excitation (500 mW) of a Nd:YAG laser.

**(III) NMR Spectroscopy.** $^1H$, $^{19}F$, and $^{11}B$ NMR spectra were recorded at room temperature on a Bruker Avance DRX-300 spectrometer operating at 300.13, 282.41, or 96.29 MHz for $^1H$, $^{19}F$, and $^{11}B$ nuclei, respectively. $^{13}C$ and $^{15}N$ NMR spectroscopic studies were performed at room temperature on a Bruker Avance DRX-500 spectrometer, operating at 125.758 or 50.678 MHz for $^{13}C$ and $^{15}N$ nuclei, respectively. The NMR signals were referenced against TMS and $CFCl_3$ as internal standards and $BF_3{\cdot}OEt_2$ in $CD_3CN$ and $MeNO_2$ in $CD_3CN$ as external standards. Concentrations of the investigated samples were in the range 0.1−1 mol L$^{-1}$. $^{15}N$ NMR spectra were obtained by direct measurements or for compounds with hydrogen available for polarization transfer with the INEPT method.[32,33] $(CF_3)_3BNCH$ samples for NMR spectroscopic studies were prepared in 5 mm NMR tubes, equipped with special valves with PTFE stems (Young, London),[34] and dry $CD_2Cl_2$ was used as solvent. Salts were dissolved in $CD_3CN$ and transferred into 5 mm o.d. NMR tubes and investigated at room temperature. Spin−lattice relaxation times, $T_1$, were determined by the inversion recovery experiment.[35] Long-range coupling constants of $^{19}F$ and isotopic shifts $^1\Delta^{19}F(^{12/13}C)$ were obtained from $^{19}F\{^{11}B\}$ spectra.

**(IV) DSC Measurements.** Thermoanalytical measurements were made with a Netzsch DSC204 instrument. Temperature and sensitivity calibrations in the temperature range of 20−500 °C were carried out with naphthalene, benzoic acid, $KNO_3$, $AgNO_3$, $LiNO_3$, and CsCl. About 5−10 mg of the solid samples were weighed and contained in sealed aluminum crucibles. They were studied in the temperature range 20−500 °C with a heating rate of 5 K min$^{-1}$; throughout this process the furnace was flushed with dry nitrogen. For the evaluation of the output, the Netzsch Protens4.0 software was employed.

The uncertainty of the enthalpies determined by DSC measurements is estimated to be 10%, mainly due to weight errors of the samples; the samples were prepared inside a glovebox to exclude moisture.

**(V) Computational Calculations.** Quantum chemical calculations were performed to support the interpretation of the experimental results in this study. DFT calculations[36] were carried out using Becke's three-parameter hybrid functional and the Lee−Yang−Parr correlation functional (B3LYP)[37−39] with the Gaussian 98 program suite.[40] Geometries were optimized and energies were calculated with the 6-311++G(d) basis set, and all structures represent true minima on the respective hypersurface (no imaginary frequency). Diffuse functions were incorporated because improved energies are obtained for anions.[41] Transition states exhibit one imaginary frequency, and IRC calculations were performed to verify that the transition states connect products and reactants, respectively.[42,43] All energies presented herein are zero-point corrected, and for enthalpies and free energies the thermal contributions are included for 298 K.

## Results and Discussion

**Synthetic Aspects.** In analogy to the reaction of $(CF_3)_3BCO$ with acetonitrile,[20,21] the reaction with HCN proceeds under ligand exchange yielding $(CF_3)_3BNCH$ and CO as


(28) Sheldrick, G. M. *SHELXS-97, Program for Crystal Structure Solution*; University of Göttingen, Germany, 1997.
(29) Sheldrick, G. M. *SHELXL-97, Program for Crystal Structure Refinement*; University of Göttingen, Germany, 1997.
(30) Otwinowski, Z.; Minor, W. *Methods Enzymol.* **1997**, *276*, 307.
(31) *Diamond-Visual Crystal Structure Information System*, ver. 2.1, 1996−1999.
(32) Morris, G. A.; Freeman, R. *J. Am. Chem. Soc.* **1979**, *101*, 760.
(33) Witanowski, M.; Stefaniak, L.; Webb, G. A. *Annu. Rep. NMR Spectrosc.* **1986**, *18*, 1.
(34) Gombler, W.; Willner, H. *International Laboratory* **1984**, 84.
(35) Berger, S.; Braun, S. *200 and More NMR Experiments*; Wiley-VCH Verlag GmbH & Co. KGaA: Weinheim, Germany, 1998.
(36) Kohn, W.; Sham, L. J. *Phys. Rev. A* **1965**, *140*, 1133.
(37) Becke, A. D. *Phys. Rev. B: Condens. Matter* **1988**, *38*, 3098.
(38) Becke, A. D. *J. Chem. Phys.* **1993**, *98*, 5648.
(39) Lee, C.; Yang, W.; Parr, R. G. *Phys. Rev. B: Condens. Matter* **1988**, *41*, 785.
(40) Frisch, M. J.; et al. *GAUSSIAN98* (revision A.6); Gaussian, Inc.: Pittsburgh, PA, 1998.
(41) Rienstra-Kiracofe, J. C.; Tschumper, G. S.; Schaefer, H. F., III; Nandi, S.; Ellison, G. B. *Chem. Rev.* **2002**, *102*, 231.
(42) Gonzales, C.; Schlegel, H. B. *J. Chem. Phys.* **1989**, *90*, 2154.
(43) Gonzales, C.; Schlegel, H. B. *J. Phys. Chem.* **1990**, *94*, 5523.

sole products according to eq 2.

$$(CF_3)_3BCO + HCN \xrightarrow[-80\ °C \rightarrow rt]{CH_2Cl_2} (CF_3)_3BNCH + CO \quad (2)$$

The isocyanotris(trifluoromethyl)borate anion, $[(CF_3)_3BNC]^-$, is accessible by deprotonation of $(CF_3)_3BNCH$ with $Li[N(SiMe_3)_2]$ in toluene (eq 3).

$$(CF_3)_3BNCH_{(solv)} + Li[N(SiMe_3)_2]_{(solv)} \xrightarrow[-20\ °C \rightarrow rt]{toluene} Li[(CF_3)_3BNC]_{(s)} + HN\{Si(CH_3)_3\}_{2(solv)} \quad (3)$$

The deprotonation of $(CF_3)_3BNCH$ with $KOH/H_2O$ fails, since the borate anion $[(CF_3)_3BNC]^-$ reacts with $(CF_3)_3BNCH$ to a complex product mixture. In contrast $Li[N(SiMe_3)_2]$ in toluene (eq 3) forms insoluble $Li[(CF_3)_3BNC]$, and no side reactions can occur. A discussion about the deprotonation reactions performed in $H_2O$ or other solvents and a detailed spectroscopic characterization of their products will be reported elsewhere. $Li[(CF_3)_3BNC]$ is converted into the potassium salt by treatment with an aqueous $KOH/K_2CO_3$ solution. The $[(CF_3)_3BNC]^-$ anion is stable under neutral as well as basic conditions, while in acidic media decomposition occurs. The main product of the acidic hydrolysis of $K[(CF_3)_3BNC]$ is $K[(CF_3)_3BNHC(O)H]$ according to eq 4.

$$K[(CF_3)_3BNC] + H_2O \xrightarrow{HCl/H_2O} K[(CF_3)_3BNHC(O)H] \quad (4)$$

In the first step the $[(CF_3)_3BNC]^-$ anion is protonated; then water reacts with the intermediate $(CF_3)_3BNCH$. The formation of $K[(CF_3)_3BNHC(O)H]$ is the reverse process of the most common isonitrile synthesis, the dehydration of *N*-substituted formamides.[44,45] Attempts to reconvert $K[(CF_3)_3BNHC(O)H]$ into $K[(CF_3)_3BNC]$ by treatment with phosgene failed, probably due to the Brønsted acidity of $(CF_3)_3BNCH$. In contrast *o*-$C_2B_{10}H_2$-3-NHC(O)H is dehydrated to *o*-$C_2B_{10}H_2$-3-NC using $POCl_3$,[11] and $K[(CF_3)_3BNHC(O)Me]$ is easily transformed into $(CF_3)_3BNCMe$ employing $P_4O_{10}$.[46]

At temperatures above 150 °C $K[(CF_3)_3BNC]$ isomerizes according to DSC measurements to the corresponding cyanoborate (eq 5).

$$K[(CF_3)_3BNC] \xrightarrow{\Delta} K[(CF_3)_3BCN] \quad (5)$$

On a preparative scale the reactions were performed at 220 °C to ensure complete isomerization within minutes (see Experimental Section). In the area of boron chemistry similar isomerizations have been reported only for *o*-$C_2B_{10}H_{11}$-3-NC[11] and $[H_nB(NC)_{4-n}]^-$ ($n = 1, 2$).[3] Similar to the $[B(CN)_4]^-$ anion[5] and in contrast to $[(CF_3)_3BNC]^-$, no hydrolysis of the $[(CF_3)_3BCN]^-$ anion in concentrated hydrochloric acid is observed.

The formation of $[(CF_3)_3BCN]^-$ as an intermediate was observed during the fluorination of $[NH_4][B(CN)_4]$ yielding $[B(CF_3)_4]^-$.[47] Currently we are optimizing the synthesis of $K[(CF_3)_3BCN]$ employing $Na[B(CN)_4]$ and 3 equiv of $ClF_3$ in anhydrous HF as starting materials. Alternative methods for the synthesis of salts with the $[(CF_3)_3BCN]^-$ anion are (i) the reaction of either $(CF_3)_3BCO$[21] or $K[(CF_3)_3BC(O)F]$[23] with ammonia yielding salts of the $[(CF_3)_3BC(O)NH_2]^-$ anion which are subsequently dehydrated employing phosgene (eq 6)

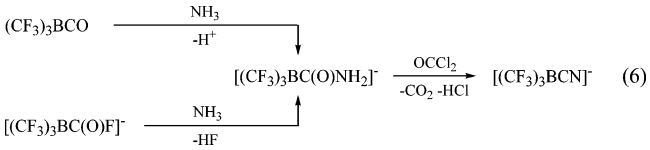

(6)

and (ii) the reactions of $(CF_3)_3BCO$ or of $[(CF_3)_3BC(O)Hal]^-$ salts ($Hal$ = F, Cl)[24] with $K[N(SiMe_3)_2]$ (eq 7).

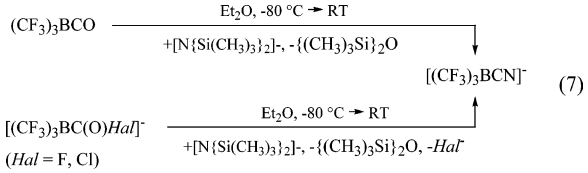

(7)

The isolated overall yields for the reactions shown in eqs 6 and 7 are lower as for the reaction sequence described herein. The reaction of $[(CF_3)_3BC(O)Cl]^-$ with $[N(SiMe_3)_2]^-$ giving $[(CF_3)_3BCN]^-$ (eq 7) is analogous to the synthesis of its higher homologues $[(CF_3)_3BCP]^-$ and $[(CF_3)_3BCAs]^-$ using $[P(SiMe_3)_2]^-$ and $[As(SiMe_3)_2]^-$, respectively.[26] Detailed descriptions of the syntheses of cyanotris(trifluoromethyl)borates as shown in eqs 6 and 7 will be given in separate contributions.

***Table 2.*** Thermal Properties of $K[(CF_3)_3BNC]$, $K[(CF_3)_3BCN]$, $K[B(CF_3)_4]$, $K[B(CN)_4]$, and $K[BF_4]$ Determined by DSC Measurements

| | phase transition | | melting point | | decomposition | | |
|---|---|---|---|---|---|---|---|
| compd | $T^a$ [°C] | $\Delta H$ [kJ mol$^{-1}$] | $T^a$ [°C] | $\Delta H$ [kJ mol$^{-1}$] | $T^a$ [°C] | $\Delta H$ [kJ mol$^{-1}$] | ref |
| $K[(CF_3)_3BNC]$ | 63 | 12 | | | 150[b] | −35[b] | *c* |
| $K[(CF_3)_3BCN]$ | 65 | 11 | 365[d] | | 370 | −200 | *c* |
| $K[BF_4]$[e] | 283 | | 460 | | | | *c* |
| $K[BF_4]$[f] | 282 | 13 | 530 | 14 | | | 8 |
| $K[B(CN)_4]$ | | | 430 | 22 | 510 | −90 | 8 |
| $K[B(CF_3)_4]$[g] | −50 | 8 | | | 320 | −90 | 47 |

[a] Onset. [b] Isomerization to $K[(CF_3)_3BCN]$. [c] This work. [d] Melts under decomposition. [e] DSC runs of the $K[(CF_3)_3BCN]$ decomposition products. [f] Other values reported: $T_{mp}$ = 530 °C,[48] 570 °C;[49] $\Delta H_{mp}$ = 18.0 kJ mol$^{-1}$;[4] $\alpha \rightarrow \beta$: 279 ± 1 °C,[48] 283 °C;[49] $\Delta H_{\alpha/\beta}$ = 13.8 kJ mol$^{-1}$.[49] [g] Further phase transition: $T$ = −65 °C, $\Delta H$ = 4.5 J g$^{-1}$.

**Thermal Properties of $K[(CF_3)_3BNC]$ and $K[(CF_3)_3BCN]$.** The thermal behaviors of the colorless salts $K[(CF_3)_3BNC]$ and $K[(CF_3)_3BCN]$ were investigated by DSC. The onset temperatures and enthalpies of the observed phase transitions, melting points, and decompositions are collected in Table 2, and the respective DSC curves are depicted in Figure 1. In addition the respective literature values for $K[BF_4]$,[8] $K[B(CN)_4]$,[8] and $K[B(CF_3)_4]$[47] are listed in Table 2. Between 60 and 70 °C, $K[(CF_3)_3BNC]$ and $K[(CF_3)_3BCN]$ reveal a reversible endothermic phase transition. In the case of $K[B(CF_3)_4]$ and of $K[(CF_3)_3BC(O)F]$ similar phase transitions were observed at −65/−50 °C[47] and at −41 °C,[24] respectively. These phase transitions are probably due to hindered rotations of the anions.

At temperatures above 150 °C, $K[(CF_3)_3BNC]$ reacts with $\Delta H_{iso} = -35 \pm 4$ kJ mol$^{-1}$ exothermically to $K[(CF_3)_3BCN]$.

(44) Ugi, I. *Isonitrile Chemistry*; Academic Press: London, UK, 1971.
(45) Grundmann, C. In *Houben-Weyl, Methoden der Organischen Chemie*; Georg Thieme Verlag: Stuttgart, 1952; Vol. E5, p 1611.
(46) Ansorge, A.; Brauer, D. J.; Bürger, H.; Krumm, B.; Pawelke, G. *J. Organomet. Chem.* **1993**, *446*, 25.
(47) Bernhardt, E.; Henkel, G.; Willner, H.; Pawelke, G.; Bürger, H. *Chem. Eur. J.* **2001**, *7*, 4696.

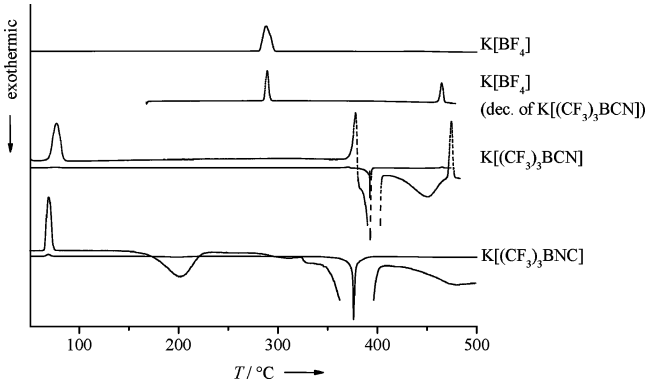


***Figure 1.*** DSC curves of K[$(CF_3)_3$BCN], K[$(CF_3)_3$BNC], and K[$BF_4$].

***Table 3.*** Experimental and Calculated[a] Enthalpies and Activation Energies for Some Isocyanide−Cyanide Rearrangements

| | $\Delta H$(298 K) [kJ mol$^{-1}$] | | | $E_a$ [kJ mol$^{-1}$] | | |
|---|---|---|---|---|---|---|
| isocyanide | calcd[a] | expl | ref | calcd[a] | expl | ref |
| K[$(CF_3)_3$BNC] | −36.1 | −35[b] | [c] | 155.7 | 136.1 | *c* |
| $(CF_3)_3$CNC | −85.1 | n.o.[d] | | (208.9) | n.o. | |
| $[BF_3NC]^-$ | −18.5 | n.o. | | 141.3 | n.o. | |
| $CF_3NC$ | −60.8 | n.o. | | 209.6 | n.o. | |
| $[BH_3NC]^-$ | −48.9 | n.o. | | 126.2 | n.o. | |
| MeNC | −99.5 | −99.2 | 18 | 170.7 | 160.7 | 17 |
| $(CH_3)_3$SiNC | −13.3 | −16.75 | 50 | 108.5 | n.o. | |

[a] This work: B3LYP/6-311++G(d). [b] DSC measurement. [c] This work. [d] n.o. = not observed.

At 365 °C, K[$(CF_3)_3$BCN] starts to melt and decomposes in an exothermic reaction at 370 °C. Due to small impurities formed during the isomerization of K[$(CF_3)_3$BNC], the decomposition occurs at somewhat lower temperatures compared to pure K[$(CF_3)_3$BCN] (Figure 1). The monocyanoborate is thermally more stable than K[$B(CF_3)_4$] which decomposes at 320 °C[47] but is less stable than K[$B(CN)_4$] which decomposes at 510 °C.[8] The DSC curve of the decomposition products of K[$(CF_3)_3$BCN] in Figure 1 shows the peak typical for the endothermic transition of K[$BF_4$] from the orthorhombic to the cubic phase at 283 °C (Table 2).[48,49] At approximately 460 °C an additional endothermic peak is observed which can be attributed to the melting point of K[$BF_4$]. Since pure K[$BF_4$] melts at 530 °C,[8] the lower value is probably due to a mixture formed during the decomposition of K[$(CF_3)_3$BCN].

**Isomerization of K[$(CF_3)_3$BNC] to K[$(CF_3)_3$BCN].** K[$(CF_3)_3$BNC] isomerizes at temperatures higher than 150 °C exothermically to the corresponding cyanoborate. The isomerization enthalpy obtained from DSC measurements of $-35 \pm 4$ kJ mol$^{-1}$ is in excellent agreement with −36.1 kJ mol$^{-1}$ obtained from DFT calculations (B3LYP/6-311+G(d), Table 3). The close values for the solid state (experimental) and the gas phase (DFT calculations) are explained by (i) very similar packing in the solid state for K[$(CF_3)_3$BNC] and K[$(CF_3)_3$BCN] as well as (ii) an intramolecular isomerization process with a negligible influence on the bonding interactions of the $(CF_3)_3B$ fragment in the crystal lattice.

The isomerization of K[$(CF_3)_3$BNC] to K[$(CF_3)_3$BCN] was monitored at four different temperatures via Raman spectroscopy. The measured Raman intensities for $\nu$(CN) were corrected by $^{19}$F NMR spectroscopy to the molar ratios of the anions (for details see the Experimental Section). The respective plots are depicted in Figure 2. The reaction was found to be of first-order, and the activation energy, $E_a$, was calculated using Arrhenius' equation (Figure 3). The experimental value of 180 kJ mol$^{-1}$ is in good agreement with the calculated value of 155.7 kJ mol$^{-1}$ (B3LYP/6-311+G(d), Table 3). The theoretical model of an intramolecular transition state as presented in Figure 4 is consistent with the experimental results: (i) a reaction of first-order, (ii) a low deviation between calculated and experimental $E_a$, and (iii) the solid-state structures showing that an intermolecular $S_N2$ type transition state would require a different ordering of the anions.

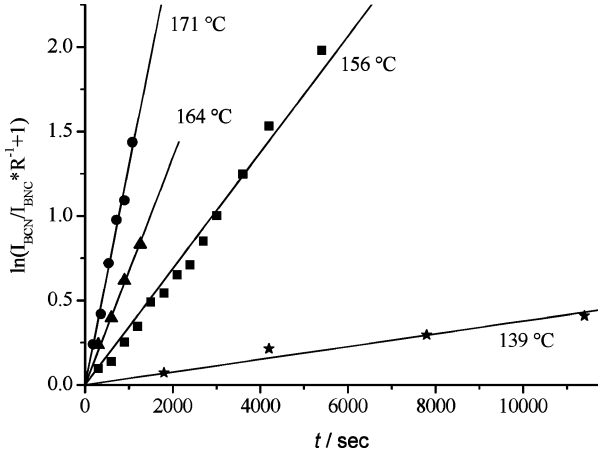


***Figure 2.*** Conversion of K[$(CF_3)_3$BNC] to K[$(CF_3)_3$BCN] at different temperatures ($R$ = 1.19 - derived from $^{19}$F NMR spectroscopy).

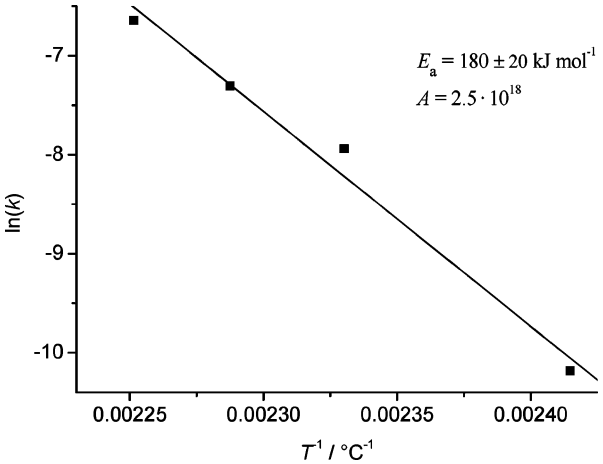


***Figure 3.*** Arrhenius plot of the isomerization of K[$(CF_3)_3$BNC] to K[$(CF_3)_3$BCN] (first-order).

The isocyanide−cyanide rearrangement presented in this contribution is analogous to isonitrile−nitrile isomerizations in organic chemistry which have been studied experimentally as well as by ab initio calculations and which are related to other 1,2-shifts, for example, Wagner−Meerwein or Beckmann rearrangements and Lewis−Zollinger isotopomerizations.[14,15] Unfortunately no direct comparison of the experimental data of $[(CF_3)_3BNC]^-$/$[(CF_3)_3BCN]^-$ with those of the isoelectronic compounds $(CF_3)_3CNC$/$(CF_3)_3CCN$ is possible because $(CF_3)_3$-CNC is so far unknown, and for $(CF_3)_3CCN$[51] no thermochemical data have been reported. The isomerization of $CF_3NC$

(48) Dworkin, A. S.; Bredig, M. A. *J. Chem. Eng. Data* **1970**, *15*, 505.
(49) Marano, R. T.; Shuster, E. R. *Thermochim. Acta* **1970**, *1*, 521.
(50) Booth, M. R.; Fraankiss, S. G. *Spectrochim. Acta, Part A* **1970**, *26*, 859.
(51) Mares, F.; Smith, J. *J. Org. Chem.* **1976**, *41*, 1567.

***Table 4.*** Calculated[a] and Experimental Bond Parameters of $[(CF_3)_3BCN]^-$[b], $[(CF_3)_3BNC]^-$[b], and $(CF_3)_3BCO$[c]

| | $[(CF_3)_3BNC]^-$ [b] | | $[(CF_3)_3BCN]^-$ [b] | | $(CF_3)_3BCO$[c] | | |
|---|---|---|---|---|---|---|---|
| | solid state | calcd | solid state | calcd | GED | solid state | calcd |
| symmetry | $C_s$ | $C_3$ | $C_s$ | $C_3$ | $C_3$ | $C_1$ | $C_3$ |
| bond length | | | | | | | |
| C−X[d] | 1.154(2) | 1.169 | 1.147(3) | 1.156 | 1.124 | 1.11(2) | 1.119 |
| B−X | 1.514(2) | 1.513 | 1.589(3) | 1.585 | 1.617(12) | 1.69(2) | 1.589 |
| B−$CF_3$ | 1.625[e] | 1.649 | 1.626[e] | 1.646 | 1.631(4) | 1.60(2) | 1.646 |
| C−F | 1.353[e] | 1.367[e] | 1.356[e] | 1.367[e] | 1.348 | 1.35 | 1.353[e] |
| bond angle | | | | | | | |
| B−N−C/B−C−N | 179.84(18) | 180.0 | 179.4(2) | 180.0 | 180.0 | 180.0 | 180.0 |
| $F_3C$−B−NC/−CN | 108.7[e] | 108.7 | 108.7[e] | 108.7 | 103.8(4) | 104.4(12) | 105.5 |
| $F_3C$−B−$CF_3$ | 110.3[e] | 110.3 | 110.3[e] | 110.3 | 114.5(4) | 114.0(12) | 113.1 |
| F−C−F | 105.1[e] | 105.3[e] | 105.1[e] | 105.2[e] | 107.2(1) | 105.7(19) | 107.3[e] |
| torsion angle | | | | | | | |
| $\tau$[f] | 1.3[e] | 8.5[e] | 1.2[e] | 7.8[e] | 11.5(9) | 16(3) | 13.0 |

[a] B3LYP/6-311++G(d). [b] $K^+$ salts. [c] Reference 21. [d] X = C or N. [e] Mean value. [f] Torsion angle from the staggered orientation of the $CF_3$ groups.

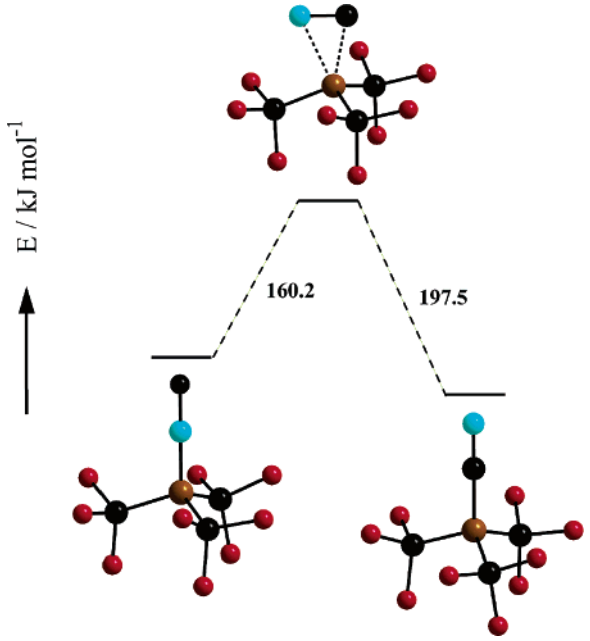


***Figure 4.*** Calculated isomerization of $K[(CF_3)_3BNC]$ to $K[(CF_3)_3BCN]$ (B3LYP/6-311+G(d)).

yielding $CF_3CN$ has not been investigated experimentally either.[52] Hence, we have included the values for the conversion of MeNC into MeCN in Table 3.[17,18] In addition the isomerizations of $(CF_3)_3CNC$ to $(CF_3)_3CCN$, $CF_3NC$ to $CF_3CN$, MeNC to MeCN, $BF_3NC$ to $BF_3CN$, and $BH_3NC$ to $BH_3CN$ were analyzed by DFT calculations (Tables 3 and S2). Furthermore for $Me_3SiNC/Me_3SiCN$ the calculated activation energy and reaction enthalpy as well as the experimental enthalpy are listed.[50,53−55] As for $[(CF_3)_3BNC]^-/[(CF_3)_3BCN]^-$ the calculated values are in good agreement with the experimental data (Table 3). For all isoelectronic examples of isonitrile−nitrile derivatives containing boron and carbon, respectively, $\Delta H$ and $E_a$ are lower for the borate anions. The lowest activation energy and reaction enthalpy are calculated for the isomerization of $Me_3SiNC$ to $Me_3SiCN$, which is in accordance with an equilibrium between $Me_3SiNC$ (0.15%) and $Me_3SiCN$ at room temperature (25 °C).[50,53−55]

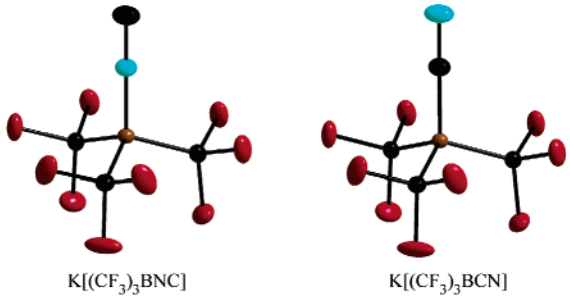


***Figure 5.*** Models of the borate anions in the solid-state structures of $K[(CF_3)_3BNC]$ and $K[(CF_3)_3BCN]$.

**Solid-State Structures of $K[(CF_3)_3BNC]$ and $K[(CF_3)_3BCN]$.** The structures of the potassium salts of $[(CF_3)_3BNC]^-$ and $[(CF_3)_3BCN]^-$ were determined by single-crystal X-ray diffraction. The obtained bond parameters are listed in Table 4; in Figure 5 models of both borate anions in the solid state are depicted, and in Figure S1 the unit cells of both structures are shown. $K[(CF_3)_3BNC]$ is the first structurally characterized isocyanoboron derivative at all, while a limited number of cyanoborates and -boranes have been investigated (Table 5). $K(CF_3)_3BNC]$ and $K[(CF_3)_3BCN]$ are isostructural and crystallize in the orthorhombic space group *Pnma*. The potassium cations in both structures are located in a mirror plane, and they show similar, weak interionic contacts[90] to nine fluorine atoms

(52) Lentz, D. *Angew. Chem.* **1994**, *106*, 1377.
(53) Booth, M. R.; Fraankiss, S. G. *J. Chem. Soc., Chem. Commun.* **1968**, 1347.
(54) Seckar, J. A.; Thayer, J. S. *Inorg. Chem.* **1976**, *15*, 501.
(55) Rasmussen, J. K.; Heilmann, S. M.; Krepski, L. R. *Advances in Silicon Chemistry* **1991**, *1*, 65.
(56) Weidlein, J.; Müller, U.; Dehnicke, K. *Schwingungsfrequenzen I Hauptgruppenelemente*; Georg Thieme Verlag: Stuttgart, 1981.
(57) Edgell, W. F.; Potter, R. M. *J. Chem. Phys.* **1956**, *24*, 80.
(58) Sano, M.; Yoshikawa, Y.; Yamatera, H. *Inorg. Chem.* **1982**, *21*, 2521.
(59) Lentz, D. *J. Fluorine Chem.* **1988**, *39*, 305.
(60) Pesek, J. J.; Mason, W. R. *Inorg. Chem.* **1979**, *18*, 924.
(61) Preetz, W.; Franken, A.; Rath, M. *Z. Naturforsch., B: Chem. Sci.* **1993**, *48*, 598.
(62) Bozorth, R. M. *J. Am. Chem. Soc.* **1922**, *44*, 317.
(63) Witanowski, M.; Stefaniak, L.; Webb, G. A. *Annu. Rep. NMR Spectrosc.* **1993**, *25*, 1.
(64) Lösking, O. *Angew. Chem.* **1989**, *101*, 1283.
(65) Olah, G. A.; Kiovsky, T. E. *J. Am. Chem. Soc.* **1968**, *90*, 4666.
(66) Buschmann, J.; Lentz, D.; Luger, P.; Perpetuo, G.; Preugschat, D.; Thrasher, J. S.; Willner, H.; Wölk, H.-J. *Z. Anorg. Allg. Chem.* **2004**, *630*, 1136.
(67) Karakida, K.; Fukuyama, T.; Kuchitsu, K. *Bull. Chem. Soc. Jpn.* **1974**, *47*, 299.
(68) Jacobs, J.; McGrady, G. S.; Willner, H.; Christen, D.; Oberhammer, H.; Zylka, P. *J. Mol. Struct.* **1991**, *245*, 275.
(69) Winnewisser, G.; Maki, A. G.; Johnson, D. R. *J. Mol. Spectrosc.* **1971**, *39*, 149.
(70) Thrasher, J. S.; Madappat, K. V. *Angew. Chem.* **1989**, *101*, 1284.
(71) Cresswell, R. A.; Robiette, A. G. *Mol. Phys.* **1978**, *36*, 869.
(72) King, C. M.; Nixon, E. R. *J. Chem. Phys.* **1968**, *48*, 1685.
(73) Dakkouri, M.; Oberhammer, H. *Z. Naturforsch., A: Phys. Sci.* **1974**, *29*, 513.
(74) Cox, P. A.; Ellis, M. C.; Legon, A. C.; Wallwork, A. *J. Chem. Soc., Dalton Trans.* **1993**, 2937.

***Table 5.*** Comparison of Structural and Spectroscopic Data of $[(CF_3)_3BCN]^-$, $[(CF_3)_3BNC]^-$, and Related Compounds

| compd | $\tilde{\nu}$ (CN) [$cm^{-1}$] | $\delta(^{11}B)$ [ppm] | $\delta(^{13}C)$ [ppm] | $\delta(^{14/15}N)$ [ppm] | $^1J(^{13}C,^{15}N)$ [Hz] | $^1J(^{11}B,^{13}C/^{15}N)$ [Hz] | $d$(C–N) [Å] | $d$(X–C/X–N)[a] [Å] | ref |
|---|---|---|---|---|---|---|---|---|---|
| $CN^-$ [b] | 2076 | | 166.2 | −100.4 | 6.1 | | 1.15 | | 56, 58, 60, 61 |
| HCN | 2098 | | 110.9 | −145 | 18.6 | | 1.1532[c] | 1.0655[c] | 56, 63, 65, 67, 68 |
| $CF_3CN$ | 2274 | | 129.0 | n.o.[d] | n.o. | | 1.1536(6)[c] | 1.4924(46)[c] | 57, 74, 76 |
| $CH_3CN$ | 2268 | | 119.6 | −137.1 | 17.5 | | 1.157[c] | 1.458[c] | 56, 65, 67, 80 |
| $[(CF_3)_3BCN]^-$ [b] | 2244 | −22.3 | 127.5 | −103.3 | 14.7 | 64.0 | 1.147(3) | 1.589(3) | *e* |
| $[H_3BCN]^-$ [f] | 2177 | −43.5 | 144.9 | n.o.[f] | n.o. | n.o. | 1.145(22)[g] | 1.486(25)[g] | 86−88 |
| $[H_2B(CN)_2]^-$ [f] | 2202 | −39.9 | 134.0 | n.o. | n.o. | n.o. | n.o. | n.o. | 3, 86 |
| $[HB(CN)_3]^-$ [f] | 2232 | −37.5 | 127.9 | n.o. | n.o. | n.o. | n.o. | n.o. | 3, 86 |
| $[B(CN)_4]^-$ [f] | 2233 | −38.5 | 122.3 | −103.0 | n.o. | 0.7 | 1.142(1) | 1.595(1) | 6, 89 |
| $[F_3BCN]^-$ [b] | 2235 | −3.8 | 131.7 | n.o. | n.o. | 90.5 | n.o. | n.o. | 7 |
| $[F_2B(CN)_2]^-$ [b] | 2231 | −7.3 | 129.1[h] | n.o. | n.o. | 80.7 | 1.142(4) | 1.604(4) | 7 |
| $[FB(CN)_3]^-$ [b] | 2230 | −17.8 | 128.0[h] | n.o. | n.o. | 77.9 | 1.136(3) | 1.605(4) | 7 |
| $[(C_6F_5)_3BCN]^-$ [i] | 2212 | −22.5 | n.o. | n.o. | n.o. | n.o. | 1.113(4) | 1.609(4) | 10 |
| $[B_6H_5CN]^{2-}$ [j] | 2149 | −24.1 | 139.0 | n.o. | n.o. | 92 | 1.1640(3) | 1.5420(3) | 61 |
| $Me_3SiCN$ | 2190 | | 127.0 | −77.7 | 11.6 | | 1.170(3)[c,k] | 1.844(7)[c,k] | 50, 73, 75, 77, 78 |
| $SF_5CN$ | 2235 | | 96.6 | n.o. | n.o. | | 1.137(5)[l,m] | 1.759(3)[l,m] | 64, 66, 82 |
| HNC | 2029 | | n.o. | n.o. | n.o. | | 1.1689[c] | 0.9940[c] | 71, 72 |
| $CF_3NC$ | 2139 | | 169.0 | −203.6 | n.o. | | 1.171(3)[c] | 1.407(3)[c] | 52, 59, 79 |
| $CH_3NC$ | 2166 | | 158.2 | −216 | 5.8 | | 1.166[c] | 1.424[c] | 81, 83−85 |
| $[(CF_3)_3BNC]^-$ [b] | 2169 | −17.5 | 172.3 | −195.4 | 9.3 | 22.9 | 1.154(2) | 1.514(2) | *e* |
| $[H_2B(NC)_2]^-$ [f] | 2165 | −21.1 | 160.9 | n.o. | n.o. | n.o. | n.o. | n.o. | 3, 86 |
| $[HB(NC)_3]^-$ [f] | 2161 | −17.3 | 165.0 | n.o. | n.o. | n.o. | n.o. | n.o. | 3, 86 |
| $Me_3SiNC$ | 2100 | | n.o. | n.o. | n.o. | | n.o. | n.o. | 50, 55 |
| $SF_5NC$ | 2080 | | 154.4 | n.o. | n.o. | | 1.158(9)[l,n] | 1.710(7)[l,n] | 66, 70, 82 |

[a] X = H, B, C, S, Si. [b] $K^+$ salt. [c] Gas phase. [d] n.o. = not observed. [e] This work. [f] $Na^+$ salt. [g] $[Au_2(dppm)_2(S_2CNEt_2)][H_3BCN]$. [h] $Li^+$ salt. [i] [K(18-Krone-6)][$(C_6F_5)_3BCN$]. [j] $Cs^+$ salt. [k] Solid: $d$(Si−C) = 1.82(3) Å, $d$(C−N) = 1.21(4) Å.[75] [l] Solid. [m] Gasphase: $d$(C−N) = 1.152(5) Å, $d$(S−C) = 1.765(5) Å.[68] [n] Second crystal: $d$(C−N) = 1.168(12) Å, $d$(S−C) = 1.698(3) Å.[66]

as well as to one carbon or nitrogen atom, respectively (Figure S2). The borate anions exhibit local $C_s$ symmetry with the linear (within experimental error) BCN/BNC fragment and one $CF_3$ group in the mirror plane. At the calculated energy minimum, $[(CF_3)_3BNC]^-$ and $[(CF_3)_3BCN]^-$ reveal $C_3$ symmetry, but the energy difference to $C_s$ symmetry is negligible with 0.2 kJ $mol^{-1}$ for both anions. The nearly linear BCN···K/BNC···K units are parallel to and stacked along the *a* axis. Alternating (180° rotated) stacks form layers in the *a*,*b* plane as presented in Figure S1.

In Table 4 calculated bond lengths and angles (B3LYP/6-311+G(d)) for $[(CF_3)_3BNC]^-$ and $[(CF_3)_3BCN]^-$ as well as experimental and theoretical values of the isoelectronic borane carbonyl $(CF_3)_3BCO$[21] and of $[B(CF_3)_4]^-$ [47] are listed. Calculated and experimental bond parameters for all tris(trifluoromethyl)-boron species are in good agreement. The difference between the measured C−N bond lengths in $[(CF_3)_3BNC]^-$ and $[(CF_3)_3BCN]^-$ is not significant, but a slightly longer bond of the isocyanide is reasonable since (i) the calculated C−N bond lengths predict the same trend, (ii) the longer $d$(C−N) for $[(CF_3)_3BNC]^-$ is in agreement with the lower $\nu$(CN) (Tables 5 and 6), and (iii) longer C−N bonds for isocyanides in comparison to the corresponding cyanides have been observed for many isocyano/cyano derivatives in organic as well as in inorganic chemistry (for selected examples see Table 5). The shorter B−N bond in $K[(CF_3)_3BNC]$ in comparison to $d$(B−C) in the cyanoborate is significant and consistent with (i) the calculated values, (ii) other isocyanide−cyanide pairs in general (Table 5), and (iii) the smaller bond radius of nitrogen in comparison to carbon.[91]

In Table 5 $d$(C−N) of selected cyanides and isocyanides are listed, and the bond lengths are very similar within the two series. Since the structures were determined by using different methods (X-ray crystallography or gas electron diffraction) and at different temperatures, a detailed comparison is omitted.

The bond lengths and angles of the $(CF_3)_3B$ groups in $[(CF_3)_3BNC]^-$ and $[(CF_3)_3BCN]^-$ are close to those in $[B(CF_3)_4]^-$ and $(CF_3)_3BCO$ and deviate only little from related tris-(trifluoromethyl)boron compounds.[23−26,92,93]

**Vibrational Spectra.** The IR and Raman spectra of $K[(CF_3)_3$-BNC] and $K[(CF_3)_3BCN]$ are depicted in Figures 6 and 7, respectively. Experimental and calculated (B3LYP/6-311+G(d)) vibrational band positions and intensities for the isotopomers $[(^{12}C^{19}F_3)_3{}^{11}B^{14}N^{12}C]^-$ and $[(^{12}C^{19}F_3)_3{}^{11}B^{12}C^{14}N]^-$ are listed in Table 6. The approximate assignment and description of modes is aided by observed and calculated isotopic shifts for the $^{10}B$ and $^{15}N$ isotopomers (Tables S4 and S5). Although $[(CF_3)_3BNC]^-$ and $[(CF_3)_3BCN]^-$ possess $C_s$ symmetry in the crystal lattice,


(75) Barrow, M. J. *Acta Crystallogr., Sect. B: Struct. Sci.* **1982**, *38*, 150.
(76) Huang, S.-G.; Rogers, M. T. *J. Chem. Phys.* **1986**, *85*, 401.
(77) Wrackmeyer, B. *Z. Naturforsch., B: Chem. Sci.* **1988**, *43*, 923.
(78) Arnold, D. E. J.; Cradock, S.; Ebsworth, E. A. V.; Murdock, J. D.; Rankin, D. W. H.; Skea, D. C. J.; Harris, R. K.; Kimber, B. J. *J. Chem. Soc., Dalton Trans.* **1981**, 1349.
(79) Christen, D.; Ramme, K.; Haas, B.; Oberhammer, H.; Lentz, D. *J. Chem. Phys.* **1984**, *80*, 4020.
(80) Kalinowski, H.-O.; Berger, S.; Braun, S. *NMR-Spektroskopie von Nichtmetallen Bd. 2 - $^{15}N$ NMR-Spektroskopie*; Georg Thieme Verlag: Stuttgart, 1992.
(81) Shimanouchi, T. *Tables of Molecular Vibrational Frequencies*; National Bureau of Standards: 1972; Vol. 1.
(82) Lentz, D. private communication.
(83) Kessler, M.; Ring, H.; Trambornio, R.; Gordy, W. *Phys. Rev.* **1950**, *79*, 54.
(84) Stephany, R. W.; De Bie, M. J. A.; Drenth, W. *Org. Magn. Reson.* **1974**, *6*, 45.
(85) Stringfellow, T. C.; Farrar, T. C. *Spectrochim. Acta, Part A* **1997**, *53*, 2425.
(86) Emri, J.; Györi, B. *Polyhedron* **1994**, *13*, 2353.
(87) Berschied, J. R.; Purcell, K. F. *Inorg. Chem.* **1970**, *9*, 624.
(88) Nazrul, I. K. M.; King, C.; Heinrich, D. D.; Fackler, J. P.; Porter, L. C. *Inorg. Chem.* **1989**, *28*, 2150.
(89) Finze, M. Diplomarbeit, Universität Hannover (Hannover, Germany), 2002.
(90) Shannon, R. D. *Acta Crystallogr., Sect. A* **1976**, *32*, 751.
(91) Pauling, L. *The Nature of the Chemical Bond and the Structure of Molecules and Crystals*, 3rd ed.; Cornell University Press: Ithaca, NY, 1960.
(92) Pawelke, G.; Bürger, H. *Coord. Chem. Rev.* **2001**, *215*, 243.
(93) Pawelke, G.; Bürger, H. *Appl. Organomet. Chem.* **1996**, *10*, 147.

***Table 6.*** Observed and Calculated[a] Band Positions and Intensities of $[(CF_3)_3BCN]^-$ and $[(CF_3)_3BNC]^-$ in the $K^+$ Salts ($^{11}B$, $^{12}C$, $^{14}N$ Isotopomers)

| $[(CF_3)_3BCN]^-$ | | | | | | | $[(CF_3)_3BNC]^-$ | | | | | | | | |
|---|---|---|---|---|---|---|---|---|---|---|---|---|---|---|---|
| $\tilde{\nu}_{calcd}$ [c] | $I_{IR}$ [d] | $I_{Ra}$ [e] | IR[c] | | Raman[c] | | $\tilde{\nu}_{calcd}$ [c] | $I_{IR}$ [d] | $I_{Ra}$ [e] | IR[c] | | Raman[c] | | assignment[b] | description of modes |
| 2312 | 3.4 | 104 | 2245 | vvw | 2244 | vs | 2210 | 168 | 91 | 2170 | vs | 2169 | vs | A $\nu_1$ | $\nu$(CN) |
| 1255 | 87 | 0.4 | 1286 | s, sh | 1286 | w, sh | 1262 | 54 | 0.1 | 1296 | s, sh | | | A $\nu_2$ | $\nu_s(CF_3)$ |
| 1236 | 480 | 9 | 1268 | vs | 1270 | m | 1245 | 389 | 10 | 1279 | vs | 1282 | m | E $\nu_{14}$ | $\nu_s(CF_3)$ |
| 1104 | 450 | 6 | 1117 | vs | 1117 | m | 1102 | 476 | 6 | 1128 | vs, br | 1116 | m | A $\nu_3$ | $\nu_{as}(CF_3)$ |
| 1082 | 444 | 5 | 1103 | vs | 1103 | w, sh | 1084 | 469 | 6 | 1098 | vs, br | 1102 | w, sh | E $\nu_{15}$ | $\nu_{as}(CF_3)$ |
| 1037 | 108 | 3.0 | 1063 | s | 1064 | w | 1037 | 96 | 2.2 | 1065 | s | 1067 | w | E $\nu_{16}$ | $\nu_{as}(CF_3)$ |
| 998 | 0.002 | 0.3 | | | | | 999 | 0.1 | 0.3 | | | | | A $\nu_4$ | $\nu_{as}(CF_3)$ |
| 963 | 241 | 2.7 | 976 | s | 976 | w | 975 | 281 | 2.4 | 987 | vs | 987 | w | A $\nu_5$ | $\nu_s$(BC/BN) |
| 883 | 324 | 1.0 | 895 | s | 900 | w | 882 | 379 | 0.8 | 894 | vs | 899 | vw | E $\nu_{17}$ | $\nu_{as}$(BC) |
| 712 | 3.8 | 10 | 723 | w | 725 | vs | 713 | 2.8 | 10 | 725 | w | 726 | vs | A $\nu_6$ | $\delta_s(CF_3)$ |
| 687 | 59 | 0.7 | 693 | s | 695 | w | 686 | 72 | 0.5 | 693 | s | 695 | w | E $\nu_{18}$ | $\delta_s(CF_3)$ |
| 540 | 0.6 | 1.2 | | | 543 | m | 539 | 0.1 | 2.4 | | | | | E $\nu_{19}$ | $\delta_{as}(CF_3)$ |
| 531 | 0.3 | 2.1 | 534 | vvw | 534 | w, sh | 535 | 0.04 | 0.8 | 540 | vw | 545 | m | A $\nu_7$ | $\delta_{as}(CF_3)$ |
| 515 | 0.01 | 0.1 | | | | | 514 | 0.01 | 0.1 | | | | | A $\nu_8$ | $\delta_{as}(CF_3)$ |
| 513 | 4.4 | 2.5 | 521 | w | 522 | m | 513 | 6 | 2.5 | 521 | m | 523 | m | E $\nu_{20}$ | $\delta_{as}(CF_3)$ |
| 433 | 12 | 0.4 | 422 | m | | | 369 | 1.9 | 0.1 | | | 366 | vw | E $\nu_{21}$ | $\delta$(BCN/BNC) |
| 392 | 1.0 | 1.4 | 413 | vw, sh | 412 | m | 407 | 1.4 | 1.1 | | | 426 | w | A $\nu_9$ | $\nu_s$(BC/BN) |
| 296 | 1.2 | 3.5 | 307 | w | 307 | s | 293 | 1.3 | 3.3 | | | 305 | s | E $\nu_{22}$ | $\rho(CF_3)$ |
| 273 | 0.3 | 2.1 | | | 291 | s | 271 | 0.6 | 1.9 | | | 290 | s | A $\nu_{10}$ | $\rho(CF_3)$ |
| 260 | 0.04 | 0.2 | 268 | vw | 268 | s | 252 | 0.1 | 2.2 | | | 260 | s | E $\nu_{23}$ | $\rho(CF_3)$ |
| 246 | 0.02 | 0.003 | 255 | vw | 255 | vvw | 245 | 0.02 | 0.003 | | | | | A $\nu_{11}$ | $\rho(CF_3)$ |
| 143 | 0.1 | 0.04 | 175 | w | | | 144 | 0.1 | 0.001 | | | | | A $\nu_{12}$ | $\delta$(CBC) |
| 135 | 4.4 | 1.4 | 151 | w, sh | 151 | w, sh | 135 | 5 | 2.1 | | | 162 | s | E $\nu_{24}$ | $\delta$(CBC) |
| 104 | 2.4 | 2.1 | 123 | w | 127 | s | 105 | 3.3 | 2.5 | | | 125 | m | E $\nu_{25}$ | $\delta$(CBC) |
| 57 | 0.3 | 0.04 | | | | | 56 | 0.3 | 0.1 | | | | | E $\nu_{26}$ | $\tau(CF_3)$ |
| 29 | 0.001 | 0.001 | | | | | 30 | 0.003 | 0.001 | | | | | A $\nu_{13}$ | $\tau(CF_3)$ |

[a] B3LYP/6-311+G(d). [b] Assignment according to $C_3$ symmetry. [c] Wavenumbers in $cm^{-1}$. [d] IR intensities in km $mol^{-1}$. [e] Raman activities in $Å^4$ $amu^{-1}$.

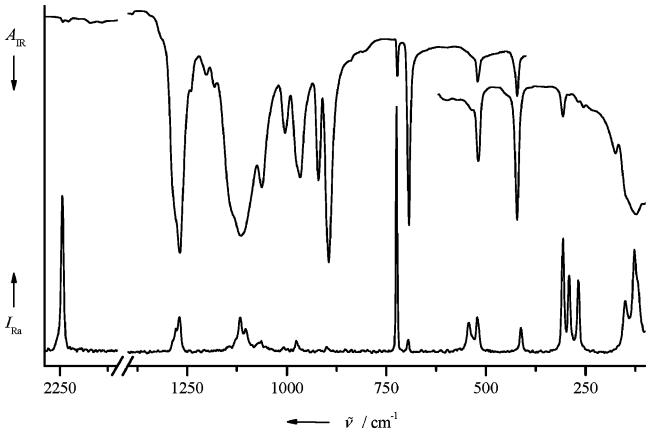


***Figure 6.*** IR and Raman spectra of $K[(CF_3)_3BCN]$.

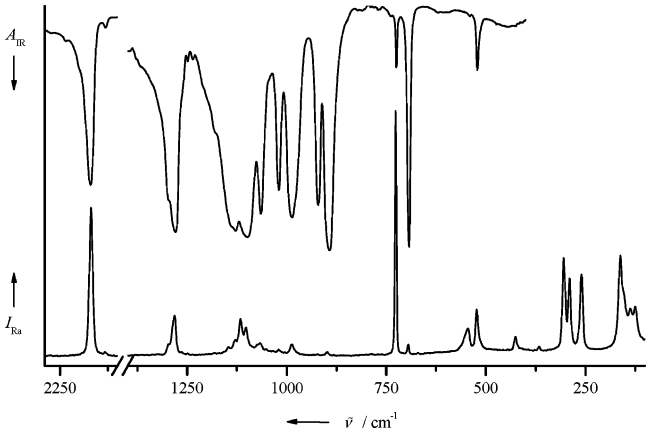


***Figure 7.*** IR and Raman spectra of $K[(CF_3)_3BNC]$.

the assignments of the band positions are in accordance to $C_3$ symmetry (eq 8) because the deviation from the ideal symmetry is very small resulting in nonmeasurable line splittings at the solid samples.

$$\Gamma_{vib} = 13\ A\ (IR, Ra\ p) + 13\ E\ (IR, Ra\ dp) \qquad (8)$$

Of the 26 vibrational fundamentals for $[(CF_3)_3BNC]^-$ and $[(CF_3)_3BCN]^-$, 20 and 22 were observed, respectively. The remaining fundamental modes either are expected to be out of the range of our spectrometer or exhibit too low intensities for detection, according to DFT calculations (Table 6).

The spectra of both borate anions display in the region from 1400 to 100 $cm^{-1}$ the band pattern typical for boranes and borate anions with $(CF_3)_3B$ groups.[21,47,92,93] Especially the IR and Raman spectra of $(CF_3)_3BCO$[21] reveal great similarities. Very characteristic are the CN stretching vibrations of $K[(CF_3)_3BNC]$ and $K[(CF_3)_3BCN]$ at 2169 and 2244 $cm^{-1}$, respectively. Higher $\nu$(CN) for cyano derivatives in comparison to their isocyano isomers are typical (Table 5) and can be reasoned by more enhanced bond strengths in the $CN^-$ ligand upon coordination via carbon than via nitrogen. To our knowledge $\nu$(CN) of the $[(CF_3)_3BCN]^-$ anion is the highest value for a CN stretching vibration of all cyanoborates known, so far. A similar but less significant trend is found for $[(CF_3)_3BNC]^-$. The high $\nu$(CN) are due to the strong Lewis acidity of tris(trifluoromethyl)-borane.[22] In analogy $(CF_3)_3BCO$ possesses the highest $\nu$(CO) 2269 $cm^{-1}$ observed for all known borane carbonyls.[21]

A definite assignment of $\nu$(B−CN) and $\nu$(B−NC) is not possible ($\nu_5$ or $\nu_9$), because these vibrational modes are strongly mixed with $\nu$(B−$CF_3$) according to calculated displacement vectors. In contrast the deformations of the BCN/BNC units can be assigned to $\nu_{21}$ at 366 $cm^{-1}$ in $[(CF_3)_3BNC]^-$ and 422 $cm^{-1}$ in $[(CF_3)_3BCN]^-$. For further assignments and descriptions

***Table 7.*** NMR Spectroscopic Data of $[(CF_3)_3BNC]^-$, $[(CF_3)_3BCN]^-$, and Related Compounds[a,b]

| parameter | $[(CF_3)_3BCN]^-$ | $[(CF_3)_3BNC]^-$ | $(CF_3)_3BNCH$ | $[B(CF_3)_4]^-$ | $[B(CN)_4]^-$ | $(CF_3)_3BCO$[c] | $[(CF_3)_3BNHC(O)H]^-$ [d] |
|---|---|---|---|---|---|---|---|
| $\delta(^1H)$ | | | 6.6 | | | | 8.1[e]/5.4[f] |
| $\delta(^{11}B)$ | −22.3 | −17.5 | −14.1 | −18.9 | −38.5 | −17.9 | −15.1 |
| $\delta(^{13}C)$ (***C***$F_3$) | 132.4 | 131.7 | 127.7 | 132.9 | | 126.2 | 133.7 |
| $\delta(^{13}C)$ (***N*C**/***C***N/***C***O) | 127.5 | 172.3 | 106.9 | | 122.3 | 159.8 | 168.8 |
| $\delta(^{15}N)$ | −103.3 | −195.4 | −210.2 | | −103.0 | | −269.3 |
| $\delta(^{19}F)$ (C***F***$_3$) | −62.1 | −67.0 | −66.6 | −61.6 | | −58.7 | −65.5 |
| $^1J(^1\boldsymbol{H},^{13}\boldsymbol{C}N)$ | | | 315.2 | | | | 188.9 |
| $^1J(^{13}\boldsymbol{C},^{15}\boldsymbol{N})$ | 14.7 | 9.3 | 50.4 | | n.o.[g] | | 11.1 |
| $^1J(^{11}\boldsymbol{B},^{13}\boldsymbol{C}F_3)$ | 76.2 | 78.4 | ∼80 | 73.4 | | 80 ± 5 | 74.9 |
| $^1J(^{11}\boldsymbol{B},^{13}\boldsymbol{C}N/^{13}\boldsymbol{C}O)$ | 64.0 | | | | 71.3 | 30 ± 5 | |
| $^1J(^{11}\boldsymbol{B},^{15}\boldsymbol{N})$ | | 22.9 | n.o. | | | | 20.7 |
| $^1J(^{13}\boldsymbol{C}F_3,C^{19}\boldsymbol{F}_3)$ | 303.2 | 304.8 | 301.1 | 304.3 | | 298.9 | 306.6 |
| $^2J(^{11}\boldsymbol{B},^{15}\boldsymbol{N})$ | n.o. | | | | 0.7 | | |
| $^2J(^{11}\boldsymbol{B},C^{19}\boldsymbol{F}_3)$ | 29.0 | 29.0 | ∼24 | 25.9 | | 36 ± 2 | 26.9 |
| $^3J(^{13}\boldsymbol{C}F_3,^{12}C^{19}\boldsymbol{F}_3)$ | 3.6 | n.o. | n.o. | 3.9 | | n.o. | n.o. |
| $^3J(^{13}\boldsymbol{C}N,^{12}C^{19}\boldsymbol{F}_3)$ | 3.5 | | | | | | n.o. |
| $^3J(^{15}\boldsymbol{N},^{19}\boldsymbol{F})$ | | | 0.6 | | | | 0.4 |
| $^4J(^{12}C^{19}\boldsymbol{F}_3,^{13}C^{19}\boldsymbol{F}_3)$ | 6.3 | 5.9 | 5.6 | 5.8 | | 6.1 | 5.9 |
| $^1\Delta^{13}C(^{10/11}B)$ (***C***$F_3$) | 0.005 | n.o. | n.o. | 0.0029 | | n.o. | 0.001 |
| $^1\Delta^{13}C(^{10/11}B)$ (***C***N) | 0.007 | | n.o. | | <0.001 | n.o. | |
| $^1\Delta^{19}F(^{12/13}C)$ | 0.1315 | 0.1300 | 0.1327 | 0.1315 | | 0.1362 | 0.1305 |
| $^2\Delta^{19}F(^{10/11}B)$ | 0.0099 | 0.0112 | n.o. | 0.0111 | | n.o. | n.o. |
| ref | *h* | *h* | *h* | 47 | 5[h] | *h* | *h* |

[a] $\delta$ and $\Delta$ in ppm, $J$ in Hz. [b] NMR solvent: $CD_3CN$. [c] NMR solvent: $CD_2Cl_2$. [d] $^1J(N^1\boldsymbol{H},^{15}\boldsymbol{N}) = 77.9$ Hz; $^2J(C(O)^1\boldsymbol{H},^{15}\boldsymbol{N}) = 16.0$ Hz; $^2J(N^1\boldsymbol{H},^{13}\boldsymbol{C}(O)) = 6.4$ Hz; $^3J(N^1\boldsymbol{H},C(O)^1\boldsymbol{H}) = 13.4$ Hz; $^5J(C(O)^1\boldsymbol{H},^{19}\boldsymbol{F}) = 0.7$ Hz. [e] $C(O)\boldsymbol{H}$. [f] $N\boldsymbol{H}$. [g] n.o. = not observed. [h] This work.

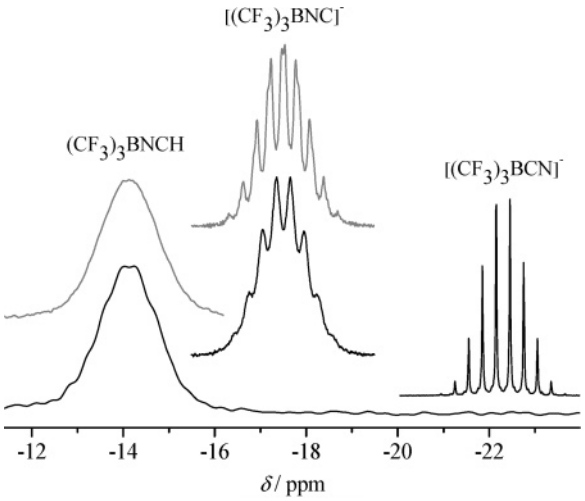


***Figure 8.*** $^{11}B$ NMR spectra of $(CF_3)_3BNCH$, $[(CF_3)_3BNC]^-$, and $[(CF_3)_3BCN]^-$ (upper traces: $(CF_3)_3B^{15}NCH$ and $[(CF_3)_3B^{15}NC]^-$).

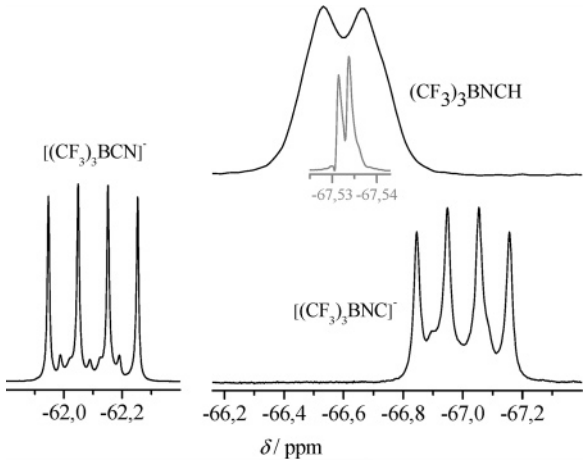


***Figure 9.*** $^{19}F$ NMR spectra of $(CF_3)_3BNCH$, $[(CF_3)_3BNC]^-$, and $[(CF_3)_3BCN]^-$ as well as $^{19}F\{^{11}B\}$ NMR spectrum of $(CF_3)_3B^{15}NCH$.

***Table 8.*** $^{11}B$ and $^{19}F$ NMR Chemical Shifts of $[(CF_3)_xB(CN)_{4-x}]^-$

| borate anion | $\delta(^{11}B)$ [ppm] | $\delta(^{19}F)$ [ppm] | ref |
|---|---|---|---|
| $[B(CF_3)_4]^-$ | −18.9 | −61.6 | 47 |
| $[(CF_3)_3BCN]^-$ | −22.3 | −62.1 | 47[a] |
| $[(CF_3)_2B(CN)_2]^-$ | −26.5 | −63.6 | 47 |
| $[CF_3B(CN)_3]^-$ | −32.0 | −65.2 | 47 |
| $[B(CN)_4]^-$ | −38.5 | | 5 |

[a] This work.

of the fundamental modes of the $(CF_3)_3B$ fragments, it is referred to the respective discussion on the isoelectronic borane carbonyl, $(CF_3)_3BCO$.[21]

The IR and Raman spectra of $(CF_3)_3BNCH$ were measured, and the most characteristic modes are the CN stretch at 2217 $cm^{-1}$ and the CH stretch at 3214 $cm^{-1}$. A detailed presentation and discussion of the spectra will be given elsewhere.

**NMR Spectra.** The isocyano- and cyanotris(trifluoromethyl)-borate anion as well as $(CF_3)_3BNCH$ were investigated by multinuclear NMR spectroscopy ($^1H$, $^{11}B$, $^{13}C$, $^{15}N$, $^{19}F$). All relevant data (chemical shifts, coupling constants, and isotopic shifts) are listed in Table 7, and for comparison the respective chemical shifts and coupling constants of $[B(CN)_4]^-$,[5] $[B(CF_3)_4]^-$, [47] and $(CF_3)_3BCO$[21] are given. The $^{11}B$ NMR spectra of the three isoelectronic species $[(CF_3)_3BCN]^-$, $[(CF_3)_3BNC]^-$, and $(CF_3)_3BNCH$ are depicted in Figure 8; in Figure 9 the respective $^{19}F$ NMR spectra are plotted. The $^{15}N$ NMR spectra of $[(CF_3)_3BCN]^-$, $[(CF_3)_3BNC]^-$, and $[B(CN)_4]^-$ are displayed in Figure S3. The $^{13}C$ NMR spectra of the novel three $(CF_3)_3B$ species are shown in Figures 10, S4, and S5, respectively.

The $^{11}B$ and $^{19}F$ NMR chemical shifts of the new boranes and borate anions are in the typical range for tetrahedrally coordinated boron compounds with three $CF_3$ groups attached to boron.[21,47,92,93] A comparison of the $^{11}B$ and $^{19}F$ NMR spectroscopic data of $[(CF_3)_xB(CN)_{4-x}]^-$ ($x = 4-0$) shows that the chemical shifts decrease with an increasing number of cyano ligands bound to boron (Table 8). For $[F_xB(CN)_{4-x}]^-$ ($x = 4-0$), an analogous trend has been reported for $\delta(^{11}B)$,[5,7] in contrast to $[H_xB(CN)_{4-x}]^-$ ($x = 4-0$)[3,5,86] (Table 5).

The $^{11}$B resonance of $[(CF_3)_3BNC]^-$ and $(CF_3)_3BNCH$ are shifted to higher frequencies compared to $[(CF_3)_3BCN]^-$, while their $\delta(^{19}F)$ values are lower. In general $(CF_3)_3B-N$ derivatives exhibit significantly higher $\delta(^{11}B)$ and lower $\delta(^{19}F)$ frequencies as compounds containing a $(CF_3)_3B-C$ fragment.[21,47,92,93]

The $^{11}$B NMR spectra of $[(CF_3)_3BNC]^-$, $[(CF_3)_3BCN]^-$, and $(CF_3)_3BNCH$ display the $^2J$ couplings to the $^{19}$F nuclei of the $CF_3$ groups, but only in the case of $[(CF_3)_3BCN]^-$ all 10 lines of the decet are observed (Figure 8). In the $^{11}$B NMR spectrum of $[(CF_3)_3BNC]^-$, only the 8 strongest lines can be seen, and for $(CF_3)_3BNCH$, the lines are nearly collapsed due to strong line broadening (Figure 8). Broad signals are typical for $^{11}$B NMR spectroscopy, and they are due to the electric field gradient at the quadrupolar $^{11}$B nucleus.[94−96] The spin−lattice relaxation times ($T_1$) as listed in Table S6 increase in the order $[(CF_3)_3BCN]^-$, $[(CF_3)_3BNC]^-$, to $(CF_3)_3BNCH$. To exclude a shortening of $T_1$, the relaxation times were also measured on $^{15}$N enriched samples. The relaxation behavior of the three isoelectronic species is controlled by quadrupolar relaxation (measured line width ($\sigma$) > 0.5−1 Hz).[21] Hence, their behavior is similar to that observed for $(CF_3)_3BCO$[21] but in contrast to that found for $[B(CF_3)_4]^-$[21,47] and $[B(CN)_4]^-$.[5] In Figure 8 also, the $^{11}$B NMR spectra of $[(CF_3)_3B^{15}NC]^-$ and $(CF_3)_3B^{15}NCH$ are depicted. The signal of $[(CF_3)_3B^{15}NC]^-$ is split into a doublet ($^1J(^{11}B,^{15}N) = 22.9$ Hz). Due to the broad lines of the $^{11}$B NMR spectrum of $(CF_3)_3BNCH$ the $^1J(^{11}B,^{15}N)$ coupling is not resolved. In the case of $[(CF_3)_3BC^{15}N]^-$, the $^2J$ coupling constant between $^{11}$B and $^{15}$N is too small to be observed. This can be rationalized, since the respective coupling constant in the $[B(CN)_4]^-$ anion, whose spectra exhibit very sharp lines (Table S6),[5] amounts to only 0.7 Hz (Table 7).

The $^{19}$F NMR spectra of $[(CF_3)_3BNC]^-$ and $[(CF_3)_3BCN]^-$ are split into quartets with lines of equal intensities due to the coupling with the $^{11}$B nucleus ($S = 3/2$) (Figure 9). The $^{19}$F NMR signal of $(CF_3)_3BNCH$ is strongly distorted due to the quadrupolar moment of the $^{11}$B nucleus. The beginning of a similar distortion is found in the case of $[(CF_3)_3BNC]^-$. This phenomenon is well-known for a nucleus A that couples with a nucleus B with a spin > $1/2$ and an inverse spin−lattice relaxation rate $\sigma_1$ (Table S6) comparable to the coupling constant $^nJ$(A,B).[21,95−97]

The $^{15}$N chemical shift of the $[(CF_3)_3BCN]^-$ anion ($\delta(^{15}N) = -103.3$ ppm) is nearly identical to the value found for $[B(CN)_4]^-$ ($\delta(^{15}N) = -103.0$ ppm)[5] and is also very similar to $\delta(^{15}N)$ of the free cyanide anion (−100.4 ppm)[58] (Table 5). As discussed for the $^{11}$B NMR spectrum of $[(CF_3)_3BCN]^-$, $^2J(^{11}B,^{15}N)$ is not resolved in the $^{15}$N NMR spectrum either (Figure S3). Smaller $^{15}$N resonance frequencies in isocyanides than in the corresponding cyanides are typical (Table 5).[33] The coupling pattern is a distorted quartet due to the interaction with the $^{11}$B nucleus (Figure S3).

The $^{13}$C NMR signals of the $CF_3$ groups in $[(CF_3)_3BNC]^-$, $[(CF_3)_3BCN]^-$, and $(CF_3)_3BNCH$ in the range from 132.4 to 127.7 ppm are split into quartets of quartets due to the couplings to $^{11}$B (relative intensity: 1:1:1:1) and to the $^{19}$F nuclei of the three fluorine atoms directly bound to the C atoms (relative intensity: 1:3:3:1) (Figures 10, S4, and S5).

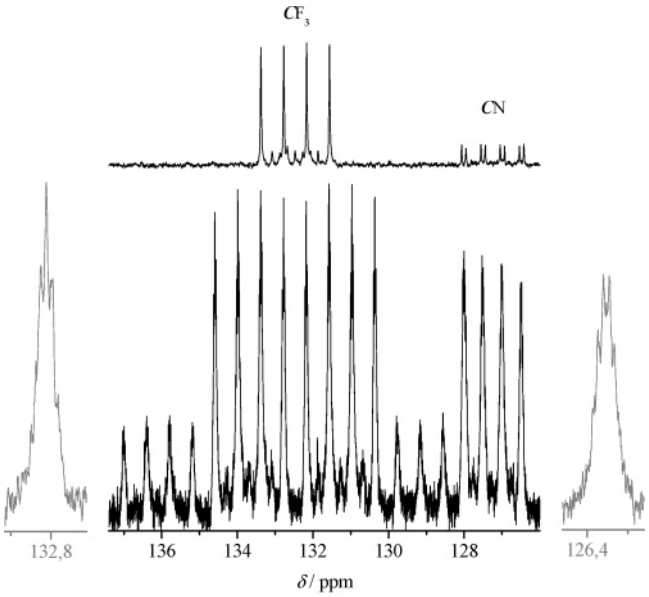


***Figure 10.*** $^{13}$C NMR spectrum of $[(CF_3)_3BCN]^-$ (bottom) and $^{13}C\{^{19}F\}$ NMR spectrum of $[(CF_3)_3BC^{15}N]^-$ (top). The expanded sections of the two signals of $[(CF_3)_3BCN]^-$ show the $^3J(^{13}C,^{19}F)$ coupling patterns.

Since the line width of the $^{13}$C NMR spectrum of $[(CF_3)_3BCN]^-$ is small, the $^3J$ coupling to the six equivalent $^{19}$F nuclei is resolved (Figure 10 and Table 7). In the $[(CF_3)_3BCN]^-$ anion, the $^1J(^{11}B,^{13}CN)$ coupling constant (64.0 Hz) is smaller than in $[B(CN)_4]^-$ (71.3 Hz), as found for $^2J(^{11}B,^{15}N)$. In $(CF_3)_3BCO$ the respective coupling constant $^1J(^{11}B,^{13}CO)$ is much smaller (30 ± 5 Hz), indicating a much stronger B−CN bond in $[(CF_3)_3BCN]^-$ compared to the B−CO bond in the borane carbonyl. The $^{13}$C NMR signal of the cyano ligand is further split into a decet due to the $^2J$ coupling between the $^{13}$C nucleus and the nine $^{19}$F nuclei.

Similar to $\delta(N^{13}C)$ in $[(CF_3)_3BNC]^-$, in $[H_xB(NC)_{4-x}]^-$ ($x = 1, 2$) the $^{13}$C resonance is shifted to higher frequencies compared to the isoelectronic cyano borate anions (Table 5).[86] For isonitriles and nitriles in organic chemistry an analogous trend is observed.[98] Due to the interaction with the proton, the $^{13}$C NMR signal of the NC group in $(CF_3)_3BNCH$ is split into a doublet. The $^{13}$C NMR spectra of the $^{15}$N labeled boron species show the respective $^1J(^{13}C,^{15}N)$ couplings. The $^1J$ coupling constant of $[(CF_3)_3BCN]^-$ ($^1J(^{13}C,^{15}N) = 14.7$ Hz) is larger than that in $[(CF_3)_3BNC]^-$ ($^1J(^{13}C,^{15}N) = 9.3$ Hz), in agreement with the C−N bond lengths and $\nu$(CN) as well as the findings for other isocyano−cyano pairs (Table 5). Due to protonation $^1J(^{13}C,^{15}N)$ is strongly increased in $(CF_3)_3BNCH$ (50.4 Hz).

The chemical shifts of $[(CF_3)_3BNHC(O)H]^-$ are listed in Table 7, and they are very similar to those reported for $[(CF_3)_3BNHC(O)Me]^-$.[46,99]

## Summary and Conclusion

The isocyanotris(trifluoromethyl)borate anion, $[(CF_3)_3BNC]^-$, is synthesized in an elegant two-step synthesis using $(CF_3)_3BCO$[20,21] as starting material. At temperatures above 150 °C,

(94) Hubbard, P. S. *J. Chem. Phys.* **1970**, *53*, 985.
(95) Halstead, T. K.; Osment, P. A.; Sanctuary, B. C.; Tagenfeldt, J.; Lowe, I. J. *J. Magn. Reson.* **1986**, *67*, 267.
(96) Wrackmeyer, B. In *Annu. Rep. NMR Spectrosc.*; Webb, G. A., Ed.; Academic Press Limited: London, U.K., 1988; Vol. 20, p 61.
(97) Abragam, A. *Principles of Nuclear Magnetism*; Clarendon Press: Oxford, 1986.
(98) Kalinowski, H.-O.; Berger, S.; Braun, S. *$^{13}$C NMR-Spektroskopie*; Georg Thieme Verlag: Stuttgart, 1984.
(99) Krumm, B. PhD Thesis, Bergische Universität Wuppertal (Wuppertal, Germany), 1991.

$K[(CF_3)_3BNC]$ isomerizes in the solid state to the corresponding cyanoborate $K[(CF_3)_3BCN]$. The reaction enthalpy and the activation energy were determined by DSC and kinetic measurements. The isomerization was modeled as an intramolecular reaction employing DFT calculations. The calculated reaction enthalpy and activation energy for the gas phase species are in good agreement with the experimental values for the solids, because no reordering of the anions in the crystal lattice is required. The intramolecular mechanism needs only slight changes in the bonding parameters of the $(CF_3)_3B$ fragment. Previous to this study two other examples for isocyanide−cyanide rearrangements in boron chemistry have been described for $[H_nB(NC)_{4-n}]^-$ ($n = 1, 2$)[3,13] and *o*-$C_2B_{10}H_{11}$-3-NC,[11,12] but for these reactions neither isomerization enthalpies nor activation energies have been determined. Hence, this study is a precedent for isocyanide−cyanide isomerizations in boron chemistry which are analogous to the well studied isonitrile−nitrile rearrangements in organic chemistry.[14,15]

Both anions have been fully characterized by vibrational (IR and Raman) and by multinuclear NMR spectroscopy ($^{11}B$, $^{13}C$, $^{15}N$, $^{19}F$) as well as by single-crystal X-ray diffraction, allowing a detailed comparison of the differences between an isoelectronic isocyano- and cyanoboron derivative for the first time. The similarities and differences are compared to related isocyano−cyano pairs in organic chemistry as well as to other selected examples in main group chemistry, for example, $Me_3SiNC$/$Me_3SiCN$ and $SF_5NC$/$SF_5CN$. General trends for cyanides compared to isocyanides are (i) shorter C−N bonds, (ii) higher $\nu$(CN) frequencies, (iii) larger $^1J(^{13}C,^{15}N)$ coupling constants, and (iv) smaller $\delta(^{13}C)$ as well as $\delta(^{15}N)$ chemical shifts.

The high chemical and thermal stabilities of $[(CF_3)_3BNC]^-$ and especially of $[(CF_3)_3BCN]^-$ will enable a detailed investigation of their chemistry. Of especial interest are their possible applications as ligands in transition metal chemistry, where they might be useful additions to nitrile and isonitrile ligands due to their anionic nature. Investigations in this direction are in progress.

**Acknowledgment.** Financial support by the Deutsche Forschungsgemeinschaft, DFG, is acknowledged. Furthermore, we are grateful to Merck KGaA (Darmstadt, Germany) for providing financial support and chemicals used in this study. We thank Mr. M. Zähres (University Duisburg-Essen) for performing some NMR measurements and Mrs. R. Brülls (University Duisburg-Essen) for the elemental analyses.

**Supporting Information Available:** Views of the unit cells of $K[(CF_3)_3BNC]$ and $K[(CF_3)_3BCN]$; views of the coordination spheres of the $K^+$ cations in $K[(CF_3)_3BNC]$ and $K[(CF_3)_3BCN]$; views of the $^{15}N$ NMR spectra of $[(CF_3)_3BNC]^-$ and $[(CF_3)_3BCN]^-$ as well as of $[B(CN)_4]^-$; views of the $^{13}C$ NMR spectra of $[(CF_3)_3BNC]^-$ as well as of $(CF_3)_3BNCH$; a table with the calculated energies, ZPCs, and enthalpies of all compounds; a table with the calculated energies of the transition states; a table with selected bond parameters of the isocyanides and cyanides and the respective transition states investigated by DFT calculations; two tables with observed and calculated isotopic shifts of $K[(CF_3)_3BNC]$ and $K[(CF_3)_3BCN]$ (IR and Raman spectroscopy); and a table with the spin−lattice relaxation rates. X-ray crystallographic files in CIF format have been deposited at the Cambridge Crystallographic Center under the deposition numbers CCDC-252110 for $K[(CF_3)_3BNC]$ and CCDC-252109 for $K[(CF_3)_3BCN]$. Copies of the data can be obtained free of charge on application to CCDC, 12 Union Road, Cambridge CB21EZ, UK (Fax: (+44)1223-336-033. E-mail: deposit@ccdc.cam.ac.uk). This material is free of charge via the Internet at http://pubs.acs.org.

JA0516357